Plant Physiol. (1994) 106: 1107–1114

Rapid Uptake of Aluminum into Cells of Intact Soybean Root Tips[1]

A Microanalytical Study Using Secondary Ion Mass Spectrometry

Dennis B. Lazof*, Jack G. Goldsmith, Thomas W. Rufty, and Richard W. Linton

United States Department of Agriculture-Agricultural Research Service, P.O. Box 1168, Oxford, North Carolina 27565 and Department of Crop Science, North Carolina State University, Raleigh, North Carolina 27695 (D.B.L., T.W.R.); and Department of Chemistry CB# 3290, University of North Carolina, Chapel Hill, North Carolina 27599 (J.G.G., R.W.L.)

A wide range of physiological disorders has been reported within the first few hours of exposing intact plant roots to moderate levels of Al^{3+}. Past microanalytic studies, largely limited to electron probe x-ray microanalysis, have been unable to detect intracellular Al in this time frame. This has led to the suggestion that Al exerts its effect solely from extracellular or remote tissue sites. Here, freeze-dried cryosections (10 μm thick) collected from the soybean (*Glycine max*) primary root tip (0.3–0.8 mm from the apex) were analyzed using secondary ion mass spectrometry (SIMS). The high sensitivity of SIMS for Al permitted the first direct evidence of early entry of Al into root cells. Al was found in cells of the root tip after a 30-min exposure of intact roots to 38 μM Al^{3+}. The accumulation of Al was greatest in the first 30 μm, i.e. two to three cell layers, but elevated Al levels extended at least 150 μm inward from the root edge. Intracellular Al concentrations at the root periphery were estimated to be about 70 nmol g^{-1} fresh weight. After 18 h of exposure, Al was evident throughout the root cross-section, although the rate of accumulation had slowed considerably from that during the initial 30 min. These results are consistent with the hypothesis that early effects of Al toxicity at the root apex, such as those on cell division, cell extension, or nutrient transport, involve the direct intervention of Al on cell function.

Almost 30 years ago, Clarkson reported that cell division and elongation of the onion root were inhibited within 2 to 6 h of exposure to a moderate activity of Al^{3+} (Clarkson, 1965, 1969). Since that time similar rapid effects on cell division and root elongation have been shown by others (Horst et al., 1983; Wallace and Anderson, 1984; Ownby and Popham, 1989; Ryan et al., 1992). In addition, moderate external [Al^{3+}] resulted in alterations in nutrient transport at the root tip (Miyasaka et al., 1989; Huang et al., 1992; Lazof et al., 1994b), disturbances in net current flux (Kochian and Shaff, 1991), and inhibition of the secretory activity of the root cap (Bennett et al., 1985b; Puthota et al., 1991), all within the first few hours of exposure. There is considerable evidence, then, that numerous physiological processes at the root tip are quickly disturbed when roots are exposed to Al.

The mechanistic basis for the rapid effects of Al at the root tip remains obscure. It is uncertain whether Al enters the root tip protoplasm and directly disrupts cell metabolism. Cell fractionation studies have suggested that this might be the case (Matsumoto et al., 1976; Niedziela and Aniol, 1983). However, alternative hypotheses have been proposed. Negative effects of Al could result from extracellular Al binding at the plasma membrane and the resulting disruption of Ca relations (Huang et al., 1992; Rengel, 1992a, 1992b), or from Al absorption at a remote site such as the root cap accompanied by signal transduction (Bennett et al., 1985a; Bennett and Breen, 1990). These alternative hypotheses have been supported by the lack of conclusive evidence that Al accumulates intracellularly within the time frame of rapid growth and metabolic effects.

The primary microanalytical method utilized for Al detection has been EPXMA. Analyses generally have indicated that the presence of Al is limited to cell walls and the root surface even after several days of exposure (Rasmussen, 1968; Huett and Menary, 1980; Marienfeld and Stelzer, 1993; Ownby, 1993). In one recent study, however, it was suggested that intracellular Al accumulation might occur within as little as 8 h (Delhaize et al., 1993). Here we bring a more sensitive microanalytical technique, SIMS, to bear on the Al accumulation question. Using cryosections of soybean (*Glycine max*) root tips, SIMS analyses clearly show substantial intracellular Al accumulation after an Al exposure of only 30 min. Direct effects of Al on cell function are possible within this time frame.

MATERIALS AND METHODS

Plant Growth and Treatment

Seeds of soybean (*Glycine max* cv Essex) were germinated for 3 d in the dark in 0.1 mM $CaSO_4$ and transferred into four

[1] This work was supported by U.S. Department of Agriculture National Research Initiative Competitive Grants Program grant No. 91-003139 (D.B.L., T.W.R., R.W.L.), Department of Energy Education Grant No. P200A10047 (J.G.G.), and a grant-in-aid from the Monsanto Corporation (R.W.L.).

* Corresponding author; fax 1-919-693-3870.

Abbreviations: EPXMA, electron probe x-ray microanalysis; SEI, secondary electron image; SEM, scanning electron microscopy; SIMS, secondary ion mass spectrometry.

90-L circulating culture systems for an additional 4 d. Light was provided by incandescent and fluorescent lights with a PPFD of 400 μmol m^{-2} s^{-1}. The nutrient solution consisted of the following (in mol m^{-3}): KH_2PO_4, 0.05; KNO_3, 0.3; $CaSO_4$, 0.4; $MgSO_4$, 0.2; and $Fe_2(SO_4)_3$, 0.005. Other micronutrients were supplied at one-quarter-strength Hoagland solution. The pH was maintained automatically at 4.2 ± 0.2 by addition of H_2SO_4. Solution temperature was 26 ± 1°C during the 12/12-h day/night cycle. On d 5, Al was added as $AlCl_3$ from fresh stock solution to produce 80 μM total Al. The calculated free Al^{3+} activity was 38 μM (GEOCHEM-PC; Parker et al., 1994). Roots of intact plants were exposed to Al for 30 min or 18 h. After exposure of roots to Al, whole plants were rinsed in ice-cold 10 mM K-citrate for 30 min to remove loosely bound Al from the root surface and cell walls (Zhang and Taylor, 1989, 1990).

For examination of growth effects, primary roots from a set of plants were put individually into open-ended plastic tubes, which tapered from a 10-mm inside diameter at the top to 4 mm near the root apex. The tubes were returned to the solution culture system and after a 2-h equilibration, plants (with tubes) were individually pulled up from the solution and the position of the root apex was marked on the outside of the tube. The position of the apex relative to the mark was noted to the nearest 10 μm using a stereomicroscope with eyepiece reticle. Plants were placed into either the control nutrient or Al treatment solution as described above. The position of the root tip relative to the original mark was recorded again after 2, 4, 6, and 24 h.

Preparation of Cryosections

Root cryosections were prepared as described in detail elsewhere (Lazof et al., 1994a). The apical 5 mm were excised with a scalpel blade, mounted on cardboard squares, quench-frozen in liquid propane (−189°C), and moved into liquid N_2. A thin band of Tissue-Tek (Miles Scientific, Elkhart, IN) was placed around the sample while it was held just over the liquid N_2 surface (about −60°C). Samples were transferred into a Reichert-Jung Frigocut-E 2000 cryostat (−35°C) and sectioned to a thickness of 10 μm using a tungsten carbide blade (Austome RTC35C, Delaware Diamond Knives, Wilmington, DE). The sections were picked up by the Tissue-Tek portion using cooled fine forceps and pressed between ultrapure indium foil (Johnson Matthey, Royston, UK) and antimony-doped ultrapure silicon wafers (MEMC, Plano, TX). Samples were then placed into divided Pyrex Petri dishes under liquid N_2, placed on a chilled (−30°C) shelf of a Virtis freeze drier (model 10–145MRBA) equipped with the Unitop 800L shelf system (Virtis, Gardiner, NY), and lyophilized for 4 d. The dried sections were stored in a vacuum desiccator until analysis in the scanning electron microscope and SIMS instrument.

SEM

To prevent charging during SEM and SIMS analyses, freeze-dried sections were sputter coated under an argon atmosphere with 10 nm of a 60/40 Au/Pd alloy using a Hummer VII sputter coater (Anatech Ltd., Alexandria, VA). Secondary electron images were obtained using an ISI DS-130 scanning electron microscope with a LaB_6 source at 8 keV potential. The printed images were used to identify the best-quality sections and regions of sections for SIMS analysis.

SIMS

The setup and operation of a secondary ion mass spectrometer has been described elsewhere (Linton et al., 1980). Here, features pertinent to interpretation in the present study are emphasized. Operation of the Cameca IMS-4f in ion microscope mode was used to directly image and localize mass signals for $^{27}Al^+$ and $^{41}K^+$ within the sample. As depicted in Figure 1, an O_2^+ primary ion beam was focused onto the specimen (S). The primary ion beam (PIB) lightly sputters the sample surface (SS), penetrating to a depth of several nanometers (PD). Neutral species, as well as positive and negative (both atomic and polyatomic) ions, are energized by the primary ion bean and those species, within a critical escape depth (ED) of a few nanometers, emerge from the sample surface. The emergent charged species originating in the specimen are "secondary ions."

In the present case, the instrument was set so that only positive secondary ions emerging from a 150-μm area of the sample surface were extracted and directed through the transfer optics (OL, TL, PL, and ES) and a double-focusing mass spectrometer (MS1 and MS2). After selection of a particular mass signal (mass:charge ratio) by the tuning of the magnetic sector (MS2), the image was projected on the dual-microchannel plate (DMCP). Mass images were digitized at each pixel by the resistive anode encoder (RAE). They could also be viewed "live," for example while positioning the specimen, by swinging the RAE aside and using a video camera (VID) to display the incoming ion signal.

For quantitation of Al, images from each specimen position were acquired under the conditions listed in Table I. To prevent RAE signal overload, low primary ion beam currents were used and $^{41}K^+$ (6.88% natural abundance) rather than the more abundant $^{39}K^+$ was imaged. Under these operating conditions, several mass images could be collected without any detectable loss of matrix as judged by post-SIMS SEM analysis and by depth profiles through similar sections at much higher beam currents (Lazof et al., 1994a). Pairs of mass images intended for quantification were collected sequentially for $^{41}K^+$ and $^{27}Al^+$ at single positions on each specimen, with acquisition periods varying from 40 to 600 s, but without further instrument adjustment or signal attenuation.

Prior to image acquisition, high mass resolution spectra for $^{41}K^+$ and $^{27}Al^+$ were obtained at a higher primary beam current to determine whether there were any species of the same nominal mass that might contribute to the overall signal. Instrument conditions were set to provide mass resolution of approximately $m/\Delta m = 4000$, sufficient to mass resolve any interferences with hydrocarbons from organic species or hydrides from inorganic species. An example of a high mass resolution spectrum is shown in Figure 2 for $^{27}Al^+$ originating from the peripheral cells of a soybean root tip. The minor peaks (<4 counts) are most likely noise rather

than mass-based signals. Similarly, there were no significant interfering signals for $^{41}K^+$. Under the conditions described in Table I, mass resolution was approximately $m/\Delta m = 1000$. The absence of significant interfering peaks was verified under these conditions by a manual mass scan prior to image collection.

Post-SIMS Analysis

Secondary ion images that had been collected under the conditions described in Table I (low beam current) were analyzed with a custom Windows-based program, yielding means and statistics for pixel-to-pixel variation within each user-defined region to be analyzed quantitatively. For each of six positions across the root radius, four discrete regions, usually including about 500 pixels each, were defined on the $^{41}K^+$ image for each image pair, due to its superior signal and structural delineation. The $^{41}K^+$:$^{27}Al^+$ ratio was automatically determined at each pixel and the mean ratio for each region was calculated. This was repeated for each of three cryosections (from three replicate plants). The resulting 12 replicate $^{41}K^+$:$^{27}Al^+$ ratios were used to compute the means and SE values (region-to-region variation). The relative sensitivity of this particular SIMS instrument for the two elements (K:Al) was determined empirically in a freeze-dried carbohydrate matrix (2.9 ± 0.3, atomic basis). By applying this factor for elemental sensitivity and a factor for the natural abundance ratios of the two isotopes (0.0688, $^{41}K^+$:$^{27}Al^+$) to the ratio of secondary ions collected and inverting the ratio, an elemental Al:K ratio was calculated.

Concentrations of Al at each position across the cryosection were estimated from the elemental Al:K ratios and analysis of K in whole 5-mm root segments by atomic emission spectroscopy. It was assumed that the K content was uniform across the root tip, as indicated previously in barley (Huang and van Steveninck, 1988). The estimates were made to indicate the approximate range of Al being detected and to facilitate comparison with previous studies. Statistical significance was considered only for the elemental Al:K ratios, which were produced from direct measurements.

Table I. *Operating conditions for low primary beam SIMS imaging*

Primary beam	
Composition	$^{16}O_2^+$ (mass filtered)
Accelerating potential	12.5 keV
Raster field	250 × 250 μm
Image field	150 μm
Beam current	<10 nA
Extraction optics	
Field aperture	1.8 mm diameter
Contrast diaphragm	20 μm
Sample offset	0 V

RESULTS

When roots of 7-d-old soybean plants are exposed to a complete nutrient solution containing 38 μM Al^{3+}, root elongation is rapidly inhibited (Fig. 3). The rate of root elongation is about 80% of the control during the 2- to 4-h interval after initial exposure to Al and decreases to about 60% during the 4- to 6-h period.

A SEI of a typical freeze-dried root tip cryosection from the region extending back 0.3 to 0.8 mm from the root apex shows the presence of undifferentiated cells with thick cytoplasm (Fig. 4). There are 20 to 25 cell layers across the root radius of 320 to 350 μm. Cell walls represent a negligible portion of the section's surface area. The possibility of vacuolar vesicles is not excluded at this distance from the apex, although the cells clearly do not have centralized vacuoles. Although some tissue is broken off and lost during freeze

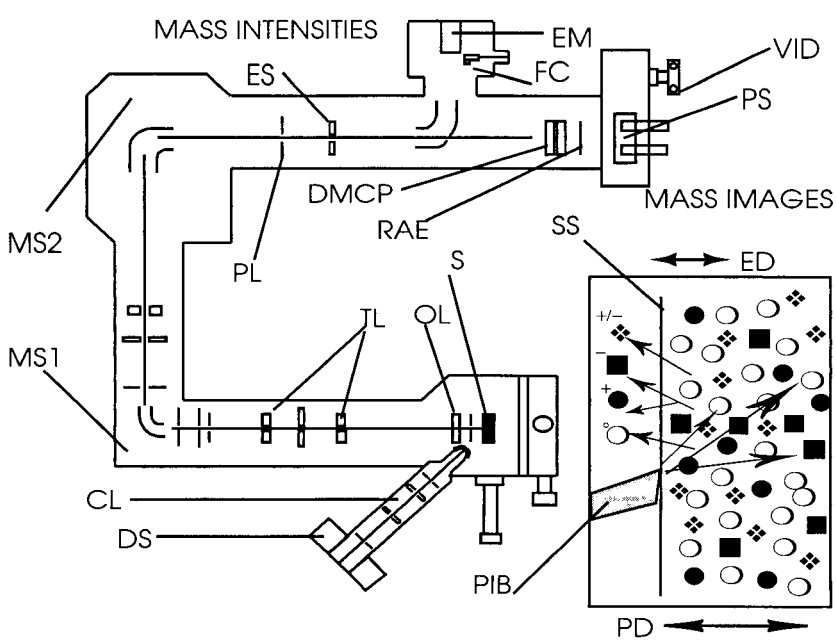

Figure 1. Principles of Cameca IMS-4F operated in ion microscope mode. DS, Duoplasmatron source; CL, condenser lenses; OL, objective lens; S, specimen; SS, sample surface; PIB, primary ion beam; PD, penetration depth; ED, escape depth; neutral (°O), positively charged (⁺●), negatively charged (⁻■) secondary ions; TL, transfer lenses; double focusing mass spectrometer MS1 and MS2 (electrostatic and magnetic sectors, respectively); PL, projection lenses; ES, exit slit; DMCP, dual microchannel plate detector; RAE, resistive anode encoder; PS, phosphorescent screen; VID, video camera; FC, Faraday cup; EM, electron multiplier.

drying, most of the section provides a suitable surface for analysis.

SIMS imaging of such cryosections indicates that substantial accumulation of Al occurs in the root tip region after 30 min of exposure to 38 μM Al^{3+} (Fig. 5). Two types of images are shown in Figure 5. In one (Fig. 5a) where a high beam current was used, an intense Al signal is evident up to 60 μm inward from the root edge, corresponding to a depth of four to five cell layers. The Al signal is concentrated in circular areas about 15 μm in diameter, similar to the size of individual cells (C1–C4). An Al signal above background extended throughout most of the image field, about 120 μm. Clusters of intense Al signal that occur deep in the root (N1–N3) were frequently observed and may represent cell nuclei on the section surface. The signals emitted outside the root originate from bits of tissue broken off during freeze drying, probably from the root edge.

In a second type of ion image, a low beam current, which would minimize beam damage and saturation of the resistive anode encoder, was used to quantitatively determine Al:K levels across the root sections (Fig. 5, b and c). The $^{27}Al^{+}$ image demonstrates the penetration of Al into the root interior, visibly extending 120 μm to the edge of the image field (Fig. 5b). As in Figure 5a, the most intense Al signal and the greatest Al signal density were located in cells at the periphery of the root. Images of native $^{41}K^{+}$ showed a different pattern, with the mass signal being more evenly distributed (Fig. 5c). Images from replicate sections similar to those shown in Figure 5, b and c, were analyzed at six positions extending radially across the root (Table II; Fig. 4, arrows). The elemental Al:K ratio decreased 5-fold from the root periphery to the root center. The intracellular Al concentration was estimated to range from 71 nmol g^{-1} fresh weight to levels undetectable with the low primary beam protocol. Control roots had Al levels below 1 nmol g^{-1} fresh weight (data not shown).

The pattern of Al accumulation across the root was examined in a similar fashion with sections from roots that had been exposed to Al for 18 h (Fig. 6). As with the 30-min Al exposure, the most intense Al signal was in cell layers at the root periphery, although penetration of Al was apparent deep into the root tissue (Fig. 6a). The relative distribution of Al, as indicated by the Al:K ratios, was only slightly different after 18 h than after 30 min, decreasing 83% from the root periphery to the root center (Table III). However, the estimated levels of Al were much greater ranging, from 355 to 62 nmol g^{-1} fresh weight. The rates of Al accumulation at all positions across the root were much slower during the latter 17.5 h than during the initial 30 min of Al exposure (Table IV).

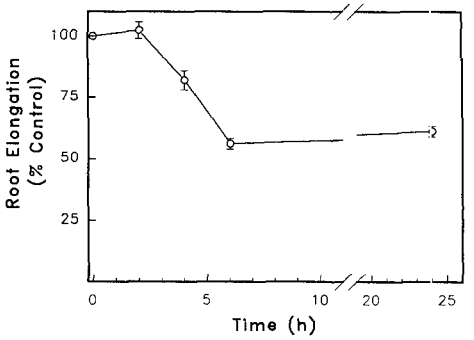

Figure 3. The inhibition of root elongation in an Al-sensitive soybean cultivar by 38 μM Al^{3+}. The elongation rate is presented as percent of the control rate. Symbols are shown at the ends of the time intervals during which each rate was measured. Error bars are SE values of the mean (n = 8).

DISCUSSION

The main objective of this study was to determine whether Al accumulated intracellularly during a brief exposure period.

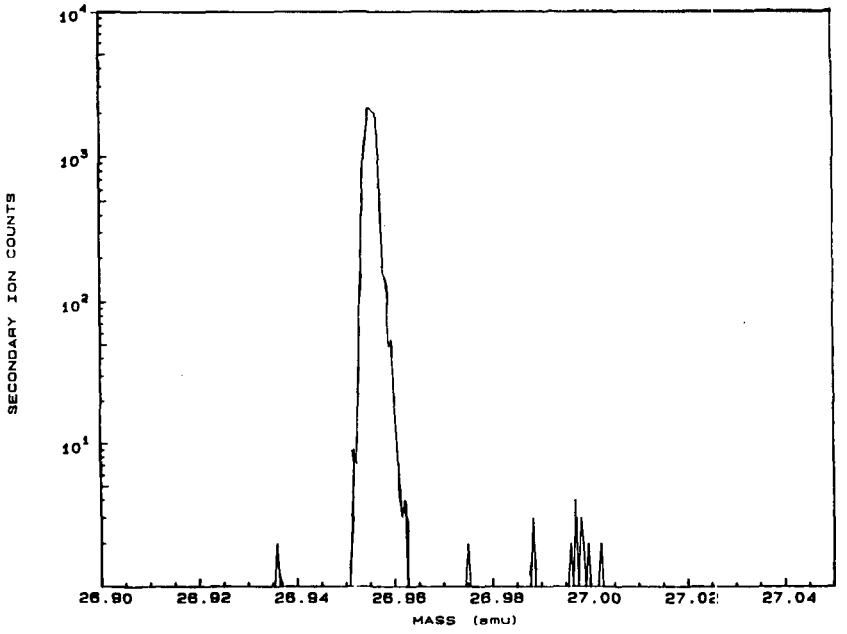

Figure 2. High mass resolution spectrum from the peripheral cells of a soybean root cryosection. The root had been exposed to Al for 30 min and given a 30-min rinse in ice-cold K-citrate. The primary beam current was set to 100 nA and the spectrum was collected for 5 min.

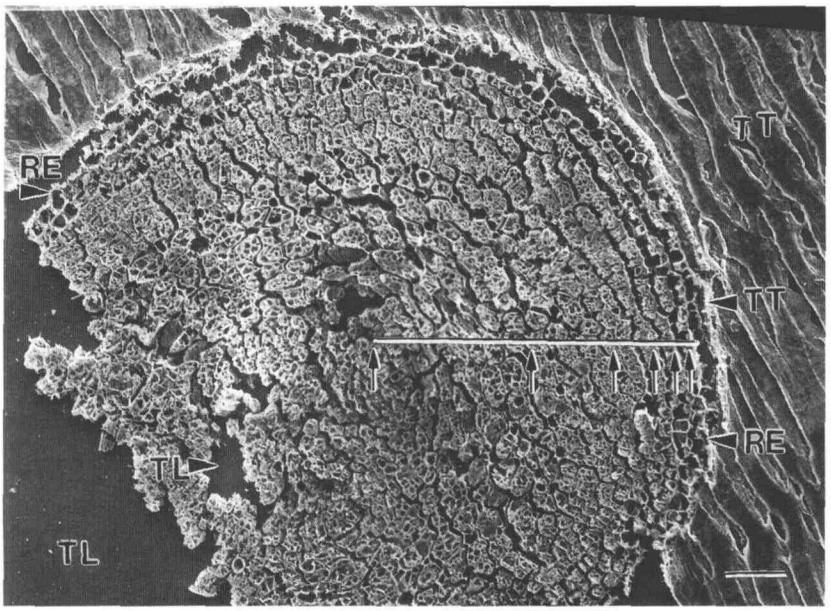

Figure 4. A scanning electron micrograph of a representative freeze-dried cryosection of soybean root tip (0.3–0.8 mm from the apex). Large arrowheads indicate Tissue-Tek (TT; the external embedment material), the root edge or protoderm (RE), and the area where tissue was lost during freeze drying (TL). The arrows along the radial line indicate the centers of positions analyzed within SIMS images during computer-based post-SIMS analysis. Bar = 50 μm (lower right).

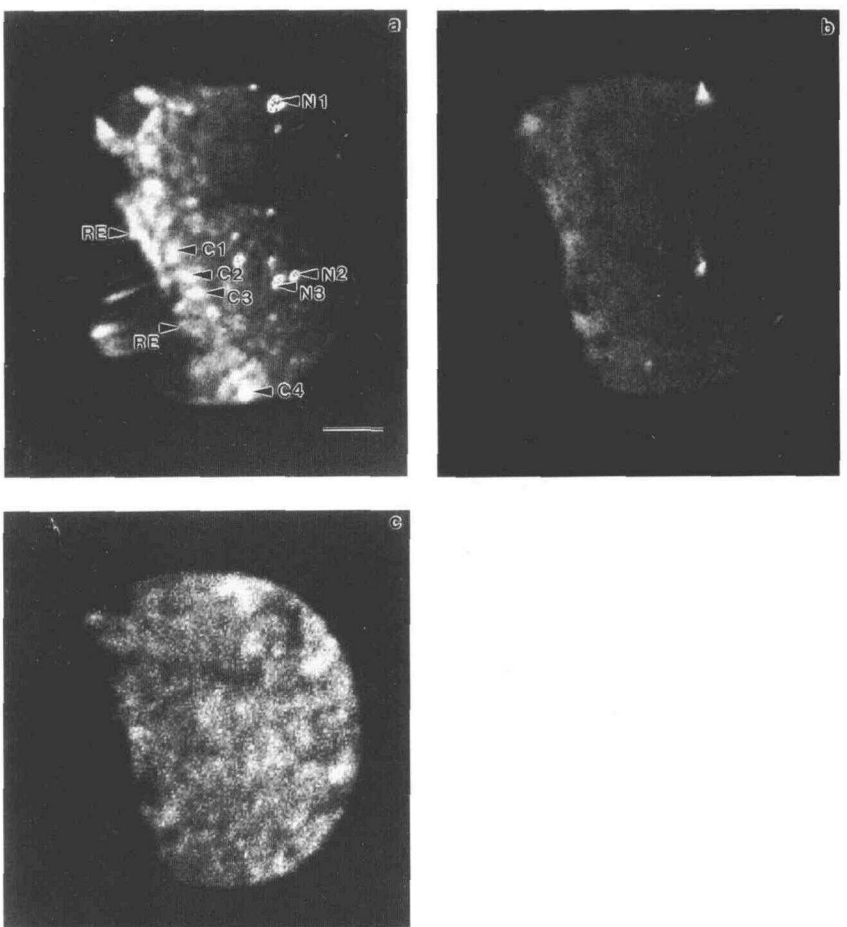

Figure 5. Secondary ion images from the periphery of a freeze-dried cryosection of soybean root after a 30-min exposure to 38 μM Al^{3+}. A high-beam current (100 nA) image for the secondary mass $^{27}Al^{+}$ is shown (a) along with two mass images collected with low-beam current (8 nA) for $^{27}Al^{+}$ (b) and $^{41}K^{+}$ (c). The images in a, b, and c were collected for 40, 600, and 40 s, respectively. Shown are mass signal groupings corresponding to individual cells in the second cell layer (from edge) of the section (C1–C4), mass signal clusters that may correspond to cell nuclei on the section surface (N1–N3) and the root edge (RE). Scale and position on section are identical in a, b, and c. Images were enhanced for photographic reproduction. Bar = 25 μm.

Table II. *The elemental Al:K ratio and Al concentration at six positions across the root tip cross-section*

Roots of intact plants were exposed to 38 μM Al^{3+} for 30 min and then rinsed for 30 min in ice-cold K-citrate (10 mM). The positions analyzed are designated by the distance from the root edge to the position center (arrows in Fig. 4). The mean values for the elemental Al:K ratio are based on 12 replicate determinations (3 replicate roots × 4 discrete determinations). The SE is given below the mean values. Values are given for Al concentrations based on the K concentration in the 0- to 5-mm root tip segment (25.3 μmol/g fresh weight). The K counts averaged 195 ± 7 (SE) per 100 pixels for the six positions. Aluminum not detectable with the low primary beam current protocol is signified as ND.

Distance from Edge of Root	Al:K/10^5	[Al] (nmol/g fresh wt)
5.0 μm	282	71.3
	41	
15 μm	233	59.0
	35	
30 μm	215	54.5
	15	
60 μm	109	27.6
	14	
150 μm	41	10.3
	13	
320–350 μm	ND	ND

The SIMS images clearly indicate that substantial amounts of Al accumulated in the root tip of soybean during a 30-min exposure to 38 μM Al^{3+}. The strongest Al signal was at the root periphery, but elevated Al also extended toward the center of the root. A large majority of the Al signal evidently was intracellular. From the SEI it is apparent that cells in this root region are relatively densely packed, with cell walls comprising a very small portion of the total volume (Fig. 4). Also, a K-citrate rinse procedure was used to remove Al from cell walls and intercellular spaces. SIMS images obtained with a high-beam current indicated signal groupings corresponding with individual cells (Fig. 5a, C1–C4). Certainly, there was no indication of "rings" of signal intensity, which would be the case if a large portion of the Al were present in the cell walls.

Other studies, using less-direct analytical methods, have also indicated that Al can accumulate intracellularly with short-term Al exposures. The experiments of Zhang and Taylor (1989, 1990) suggested considerable Al accumulation in the symplasm of 5-mm wheat root tips with an Al exposure of 30 min. From their data it can be estimated that Al concentrations were in the range of 400 nmol g^{-1} fresh weight h^{-1}, slightly greater than the concentrations estimated here (Tables II and III). After the citrate rinsing procedure of Zhang and Taylor for removal of apoplastic Al, we found that a 2-h Al exposure resulted in an accumulation of Al of about 300 nmol g^{-1} fresh weight h^{-1} in whole 0- to 5-mm root tips of soybean (Lazof et al., 1994b). Furthermore, it was shown in cell-fractionation studies that exposure of pea roots to a relatively high concentration of Al (1 mM) resulted in considerable Al entry into cells and binding to nucleic acids within the initial 5 to 8 h of exposure (Matsumoto et al., 1976).

It does appear, then, that the time frame of intracellular Al accumulation at nanomolar levels coincides with that of the earliest reported toxicity responses. The rapid Al toxicity effect may be localized primarily at the root tip (Clarkson, 1969; Bennett et al., 1985a; Kochian and Shaff, 1991). Applying agar blocks along a length of root, Ryan et al. (1993) defined the critical site of Al exposure as the apical 2 to 3 mm in wheat. The cryosections analyzed by SIMS in our studies were obtained from the root zone located 0.3 to 0.8 mm basipetal from the tip. This is a transitional zone for cell division and extension. The implication is that the Al penetration into the zone could directly interfere with both processes. It is necessary to interject caution, however, with this line of reasoning. The concentration of Al required for toxic

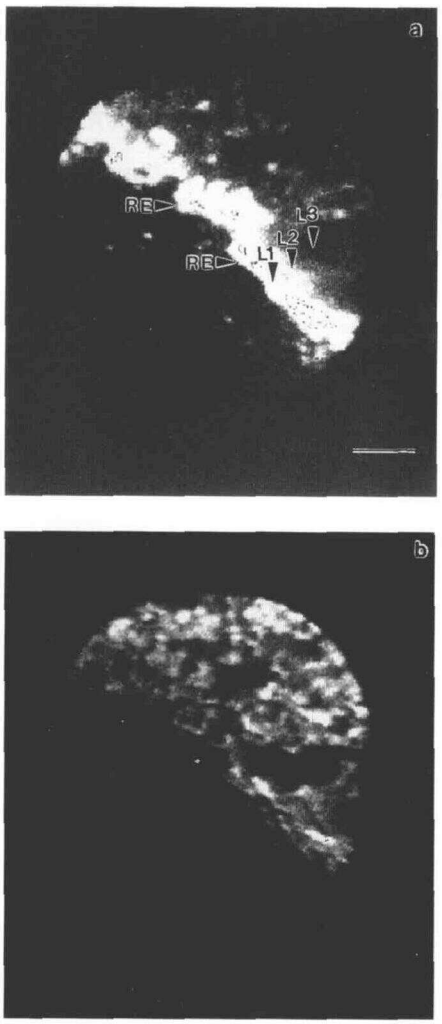

Figure 6. Secondary ion images from the periphery of a freeze-dried cryosection of soybean root tip after an 18-h exposure to 38 μM Al^{3+}. Shown are the low-beam current mass images for $^{27}Al^+$ (a) and $^{41}K^+$ (b). The SIMS images were collected (40 s each) under the conditions described in Table I (at low beam current) and so demonstrate the images of the type appropriate for mass ratioing and computer-assisted quantification. Arrowheads indicate first, second, and third cell layers (L1–L3) inwards from root edge (RE). Sublimed position [illegible] identical in a and b. Bar = 25 μm.

Table III. *The elemental Al:K ratio at six positions across the root tip cross-section*

Roots of intact plants were exposed to 38 μM (Al^{3+}) for 18 h and then rinsed for 30 min in ice-cold K-citrate. Details are as for Table II. The K counts averaged 262 ± 4.

Distance from Edge of Root	Al:K/10^5	[Al] (nmol/g fresh wt)
5.0 μm	1405	355
	148	
15 μm	778	197
	109	
30 μm	511	129
	106	
60 μm	529	134
	35	
150 μm	482	122
	44	
320–350 μm	243	62
	12	

effects in a cellular environment is unknown, as is the extent to which speciation and binding might render Al benign inside the cell. The possibility of important Al effects at the extracellular surface of the plasma membrane (Huang et al., 1992; Rengel, 1992a, 1992b; Kinraide et al., 1993), of course, cannot be excluded.

Much of the controversy surrounding the question of Al accumulation in root cells stems from investigations using EPXMA that have generally failed to detect intracellular Al after short-term Al exposures (Rengel, 1992b). This is due mainly to sensitivity limitations. For example, Marienfeld and Stelzer (1993) recently found that intracellular Al was not detectable after a 1-d exposure of oat roots but was detectable after 10 d. They estimated a detection limit of 2 to 3 μmol g^{-1} fresh weight in their frozen-hydrated specimens. This lowest detectable level is about 2 orders of magnitude more than amounts we measured here with SIMS operating under the low-beam current conditions for optimal quantitation (Tables II and III). It should be noted that there is an additional 50-fold improvement in SIMS sensitivity for Al at higher-beam currents (about 100 nA; data not shown).

Another important limitation with EPXMA is spatial resolution. In a recent EPXMA study, Delhaize et al. (1993) suggested that intracellular Al was detected in wheat root tips after their "prolonged exposures," i.e. 8- and 24-h treatments. In the 8-h Al treatment, root levels were 5 mg g^{-1} dry weight (about 10 μmol g^{-1} fresh weight). By analyzing freeze-dried samples, sensitivity was increased 10-fold (Lazof and Lauchli, 1991). Evidently, this improvement was sufficient to allow detection of Al in wheat root tips after the 8-h exposure. Problems in interpretation arise, however, in part due to the limitations in spatial resolution with EPXMA analysis of freeze-dried bulk samples. The depth resolution in freeze-dried biological tissue lies between 40 and 60 μm (Boekestein et al., 1980, assuming 90% initial water content). Given the teardrop-shaped volume of electron beam/specimen interaction and the low x-ray absorbance of soft tissue, the lateral resolution would be of about the same magnitude as the depth resolution (Goldstein et al., 1981). As a result, the minimal limit of lateral resolution was much larger than the diameter of individual cells examined (figure 9 of Delhaize et al., 1993). The situation is further complicated by the use of a distilled water rinse after the Al exposure period. Aluminum in the cell wall was retained, which can account for 40 to 70% of the total Al present (Zhang and Taylor, 1989; Tice et al., 1992). Under such circumstances it would seem unlikely that an intracellular Al component was resolved in the Delhaize study.

A high degree of spatial resolution was possible in our experiments employing the SIMS approach. The use of cryosections was critical. Most of the cell contents dry vertically onto the underlying substrate during freeze drying, with minimal movement of cytoplasm into the cell wall (Lazof et al., 1994a). Cryosectioning prevents the loss of soluble ions during sample preparation and minimizes the opportunity for contamination of specimens with Al, a ubiquitous element. The SIMS technique itself is classed a "surface analytical" method. Under the low primary beam energy and dose used here, we have estimated the depth of primary beam damage to be on the order of 10 nm and lateral resolution to be in the 2-μm range (Lazof et al., 1994a).

Aside from the controversy of whether intracellular Al can be detected with EPXMA during the first hours of exposure, a consistent observation in EPXMA studies is that the highest Al accumulation occurs at the root periphery (Matsumoto et al., 1976; Delhaize et al., 1993; Marienfeld and Stelzer, 1993). In our study we found this to hold true when intracellular Al was detected by SIMS (Figs. 5 and 6; Tables II and III). The SIMS data also indicate a sharp decline in the Al accumulation rate in both peripheral cells and cells of the root interior as the Al exposure period was extended to 18 h (Table IV). A large decrease in the rate of symplastic Al accumulation, i.e. a shift to a slower linear uptake phase, occurred in previous experiments with wheat root tips (Zhang and Taylor, 1989). The mechanistic basis for decreased Al absorption with time of exposure remains obscure. The decreasing rate could reflect the progressive obstruction of apoplastic access to cellular absorption sites. Alternatively, the effect could represent the controlled "down-regulation" of Al entry into the root symplasm or activation of Al exclusion processes

Table IV. *Calculated Al accumulation rates in each of six positions of a root tip cross-section*

Rates were calculated from the Al accumulated in the first 30 min or subsequent 17.5 h (from data of Tables II and III). The 17.5-h rate for the innermost position assumed no Al absorption during the initial 30 min.

Distance from Edge of Root	Accumulation Rate	
	0–0.5 h	0.5–18 h
	nmol g^{-1} fresh weight h^{-1}	
5.0 μm	142	12.2
15 μm	117	4.5
30 μm	109	1.2
60 μm	55	4.5
250 μm	21	5.8
400 μm	ND	3.5

(Rincon and Gonzales, 1992). Although neither the means by which Al enters root cells nor the means by which its entry rate is slowed are known, the present study allows the possibility that early Al toxicity effects are exerted directly by intracellular Al and that tolerance mechanisms might involve the limitation of Al entry.

ACKNOWLEDGMENTS

The SIMS analysis was conducted at British Petroleum's Warrensville Research Center (Cleveland, OH) with technical assistance from S.R. Bryan and J. Gibson.

Received May 5, 1994; accepted July 10, 1994.

LITERATURE CITED

Bennet RJ, Breen CM (1990) The aluminium signal: new dimensions to mechanisms of Al tolerance. *In* RJ Wright, VC Baligar, RP Murrmann, eds, Plant-Soil Interactions at Low pH. Kluwer Academic Publishers, Dordrecht, The Netherlands, pp 24–29

Bennett RJ, Breen CM, Fey MV (1985a) Aluminium uptake sites in the primary root of *Zea mays* L. S Afr J Plant Soil **2:** 1–7

Bennett RJ, Breen CM, Fey MV (1985b) The primary site of aluminum injury in the root of *Zea mays* L. S Afr J Plant Soil **2:** 8–17

Boekestein A, Stolo ALH, Stadhouders AM (1980) Quantitation in x-ray microanalysis of biological bulk specimens. Scanning Electron Microsc **II:** 321–334

Clarkson DT (1965) The effect of aluminium and some other trivalent metal cations on cell division in the root apices of *Allium cepa*. Ann Bot **29:** 309–315

Clarkson DT (1969) Metabolic aspects of aluminium toxicity and some possible mechanisms for resistance. *In* IH Rorison, ed, British Ecological Society Symposium No. 9. Blackwell Scientific Publishers, Oxford, UK, pp 381–397

Delhaize E, Craig S, Beaton CD, Bennet RJ, Jagadish VC, Randall PJ (1993) Aluminum tolerance in wheat (*Triticum aestivum* L.). I. Uptake and distribution of aluminum in root apices. Plant Physiol **103:** 685–693

Goldstein JI, Newbury DE, Echlin P, Joy DC, Fiori C, Lifshin E (1981) Practical techniques of x-ray analysis. *In* JI Goldstein, DE Newbury, P Echlin, DC Joy, C Fiori, E Lifshin, eds, Scanning Electron Microscopy and X-Ray Microanalysis. Plenum Press, New York, pp 393–446

Horst WJ, Wagner A, Marschner H (1983) Effect of aluminum on root growth, cell-division rate and mineral element contents in roots of *Vigna unguiculata* genotypes. Z Pflanzenphysiol **109:** 95–103

Huang CX, van Steveninck RFM (1988) Effect of moderate salinity on patterns of potassium, sodium and chloride accumulation in cells near the root tip of barley: role of differentiating metaxylem vessels. Physiol Plant **73:** 525–533

Huang JW, Shaff JE, Grunes DL, Kochian LV (1992) Aluminum effects on calcium fluxes at the root apex of aluminum-tolerant and aluminum-sensitive wheat cultivars. Plant Physiol **98:** 230–237

Huett DO, Menary RC (1980) Aluminium distribution in freeze-dried roots of cabbage, lettuce and kikuyu grass by energy-dispersive x-ray analysis. Aust J Plant Physiol **7:** 101–111

Kinraide TB, Ryan PR, Kochian LV (1993) Al^{3+}-Ca^{2+} interactions in aluminum rhizotoxicity. II. Evaluating the Ca^{2+}-displacement hypothesis. Planta **292:** 104–109

Kochian LV, Shaff JE (1991) Investigating the relationship between aluminium toxicity, root growth and root-generated ion currents. *In* RJ Wright, VC Baligar, RP Murrmann, eds, Plant-Soil Interactions at Low pH. Kluwer Academic Publishers, Dordrecht, The Netherlands, pp 769–778

Lazof DB, Goldsmith JG, Rufty TW, Suggs C, Linton RW (1994a) A method for the routine preparation of cryosections from plant tissue: suitability for secondary ion mass spectrometry. J Microsc (in press)

Lazof D, Lauchli A (1991) Complementary analysis of freeze-dried and frozen-hydrated plant tissue by electron-probe X-ray microanalysis: spectral resolution and analysis of calcium. Planta **184:** 327–333

Lazof D, Rincon M, Rufty TW, MacKown CM, Carter TE (1994b) Aluminum absorption in morphological regions of intact soybean root and associated effects on $^{15}NO_3^-$ influx. Plant Soil (in press)

Linton RW, Walker SR, DeVries CR, Ingram P, Shelburne JD (1980) Ion microanalysis of cells. Scanning Electron Microsc **1980:** 583–596

Marienfeld S, Stelzer R (1993) X-ray microanalyses in roots of Al-treated *Avena sativa* plants. J Plant Physiol **141:** 569–573

Matsumoto H, Hirasawa E, Torikai H, Takahashi E (1976) Localization of absorbed aluminium in pea root and its binding to nucleic acids. Plant Cell Physiol **17:** 127–137

Miyasaka SC, Kochian LV, Shaff JE, Foy CD (1989) Mechanisms of aluminum tolerance in wheat. Plant Physiol **91:** 1188–1196

Niedziela G, Aniol A (1983) Subcellular distribution of aluminium in wheat roots. Acta Biochim Pol **30:** 99–105.23

Ownby JD (1993) Mechanisms of reaction with aluminium-treated roots. Physiol Plant **87:** 371–380

Ownby JD, Popham HR (1989) Citrate reverses the inhibition of wheat root growth caused by aluminum. J Plant Physiol **135:** 588–591

Parker DR, Norvell WA, Chaney RL (1994) GEOCHEM-PC: a chemical speciation program for IBM and compatible personal computers. *In* RH Loeppert, ed, Chemical Equilibrium and Reaction Models. Soil Science Society of America, Madison, WI (in press)

Puthota V, Cruz-Ortega R, Johnson J, Ownby J (1991) An ultrastructural study of the inhibition of mucilage secretion in the wheat root cap by aluminium. *In* RJ Wright, VC Baligar, RP Murrmann, eds, Plant-Soil Interactions at Low pH. Kluwer Academic Publishers, Dordrecht, The Netherlands, pp 779–787

Rasmussen HP (1968) Entry and distribution of aluminum in *Zea mays*. Planta **81:** 28–37

Rengel Z (1992a) Disturbance of cell Ca^{2+} homeostasis as a primary trigger of Al toxicity syndrome. Plant Cell Environ **15:** 931–938

Rengel Z (1992b) Role of calcium in aluminium toxicity. New Phytol **121:** 499–513

Rincon M, Gonzalez RA (1992) Aluminum partitioning in intact root tips of aluminum-tolerant and -sensitive wheat (*Triticum aestivum* L.) cultivars. Reduced aluminum accumulation and rapid translocation mechanisms operate in aluminum-tolerant wheat roots. Plant Physiol **99:** 1021–1028

Ryan PR, DiTomaso JM, Kochian LV (1993) Aluminium toxicity in roots: an investigation of spatial sensitivity and the role of the root cap. J Exp Bot **44:** 437–446

Ryan PR, Shaff JE, Kochian LV (1992) Aluminum toxicity in roots. Correlation among ionic currents, ion fluxes, and root elongation in aluminum-sensitive and aluminum-tolerant wheat cultivars. Plant Physiol **99:** 1193–1200

Tice KR, Parker DR, DeMason DA (1992) Operationally defined apoplastic and symplastic aluminum fractions in root tips of aluminum-intoxicated wheat. Plant Physiol **100:** 309–318

Wallace SU, Anderson IC (1984) Aluminum toxicity and DNA synthesis in wheat roots. Agron J **76:** 5–8

Zhang G, Taylor GJ (1989) Kinetics of aluminum uptake by excised roots of aluminum tolerant and aluminum sensitive cultivars of *Triticum aestivum* L. Plant Physiol **91:** 1094–1099

Zhang G, Taylor GJ (1990) Kinetics of aluminum uptake in *Triticum aestivum* L. Plant Physiol **94:** 577–584